Applied Surface Science 635 (2023) 157740

Contents lists available at ScienceDirect

Applied Surface Science

journal homepage: www.elsevier.com/locate/apsusc

Full Length Article

Co/Pd-based spin-valves with perpendicular magnetic anisotropy on flexible substrates. Direct deposition vs transfer-and-bonding approaches

Mariam Hassan [a,b], Sara Laureti [a], Christian Rinaldi [c], Federico Fagiani [c], Gianni Barucca [a,d], Annamaria Gerardino [e], Nataliia Schmidt [b], Mario Fix [b], Manfred Albrecht [b], Gaspare Varvaro [a,*]

[a] Institute of Structure of Matter, National Research Council, nM2-Lab, Research Area Roma 1, Monterotondo Scalo (Roma), 00015, Italy
[b] Institute of Physics, University of Augsburg, Universitätsstraße 1 Nord, D-86159 Augsburg, Germany
[c] Department of Physics, Politecnico di Milano, c/o via G. Colombo 81, 20133 Milano, Italy
[d] Department SIMAU, University Politecnica delle Marche, Via Brecce Bianche, Ancona 60131, Italy
[e] Institute of Photonics and Nanotechnologies, National Research Council, Via del Fosso del Cavaliere 100, Roma, 00133, Italy

ARTICLE INFO

Keywords:
Flexible spintronics
PMA spin valves
Direct deposition
Transfer-and-bonding

ABSTRACT

Flexible spintronics is an emerging field of research that has received increasing attention due to the additional functionalities that are allowed (lightweight, flexibility, shape-ability, wearability) with respect to conventional rigid systems. In this work, different strategies for the fabrication of flexible spintronic devices with perpendicular magnetic anisotropy are compared, i.e., transfer-and-bonding approaches exploiting wet and dry lift-off methods, and direct deposition on flexible substrates. To evaluate the potential of the proposed strategies, Co/Pd-based giant magneto-resistive spin-valves including a synthetic antiferromagnet reference electrode were investigated. Such stacks represent a demanding model system, owing to the large number of interfaces whose quality strongly affects the overall magnetic and electric performances. The advantages and drawbacks of the different strategies are discussed to provide crucial indications for the development of flexible spintronic devices of any complexity. Based on the results, the most suitable option for achieving high-quality heterostructures on large area surfaces via direct deposition is using polyethylene naphthalate (Teonex®) tapes, provided that the processing and operating temperatures are relatively low (<525 K). On the other hand, if the process requires higher temperatures, the dry lift-off method exploiting the low adhesion between an Au underlayer and the SiOx/Si(100) substrate is the preferred alternative.

1. Introduction

Magnetic thin films and multilayers exhibiting spin-dependent transport phenomena have become a major field of research [1,2] since the discovery of the giant magneto-resistance (GMR) at the end of the 1980s' [3,4]. While most efforts have been focused on rigid devices, attention has been recently paid to spintronic thin film systems on flexible tapes, owing to their additional functionalities (lightweight, flexibility, shape-ability, and wearability) and potential applications in many strategic sectors, including automotive, wearable electronics, soft robotics, IoT, and bio-integrated electronics [5–7]. So far, most studies have been devoted to flexible spintronic systems with in-plane magnetic anisotropy [8–13], while only a few examples are reported on flexible structures with perpendicular magnetic anisotropy (PMA) [14–19], which are featured by an intrinsic and large uniaxial magnetic anisotropy allowing for additional functionality and improved performance (e.g., higher thermal stability and robustness against spurious magnetic fields) [20–22] that may significantly expand the range of applications of flexible spintronic devices. The limited number of studies is mainly due to the stringent constraints needed to obtain high-quality PMA spintronic thin films, requiring for a fine control of the layers' properties at the sub-nanometer level, hardly achievable on most common flexible polymeric tapes that are amorphous and have a high surface roughness.

Starting from our previous works about the fabrication of PMA GMR spin-valves (SVs) on flexible substrates [14–16], here we present additional strategies to extend the knowledge in this rapidly developing field and identify benefits and drawbacks of different approaches to guide the community to the selection of the most promising route to obtain high-quality and complex PMA spintronic systems on flexible substrates.

* Corresponding author.
E-mail address: gaspare.varvaro@ism.cnr.it (G. Varvaro).

https://doi.org/10.1016/j.apsusc.2023.157740
Received 20 April 2023; Received in revised form 1 June 2023; Accepted 6 June 2023
Available online 8 June 2023

Two general methods are usually exploited to fabricate flexible thin film electronic devices, i.e., i) *direct deposition* on flexible substrates and ii) *transfer-and-bonding* of the whole structure from a rigid substrate to a flexible tape [23,24]. The direct deposition on flexible substrates is a single-step and low-cost process that allows high-surface coverages. Commonly employed flexible substrates are polymers, including polyethylene terephthalate (PET), polyethylene naphthalate (PEN), polyethersulphone (PES) and polyimide (PI) [25]. Those are highly flexible materials, inexpensive, and compatible with the roll-to-roll processing; however, they are generally affected by a high surface roughness and a low thermal stability compared to rigid substrates, thus limiting the number of materials that can be prepared. Inorganic flexible substrates, including natural MICA sheets and ultra-thin crystalline Si wafers, have been proposed to overcome those issues [26–28]. MICA is a natural mineral whose mechanical exfoliation allows obtaining thin sheets that are atomically flat, transparent, mechanically robust, flexible (for thicknesses lower than 100 μm [20]) as well as thermally stable (up to ~800 and ~1200 K for muscovite and phlogopite, respectively [29]), thus being compatible with state-of-the-art inorganic electronic materials [26]. MICA substrates were successfully exploited for the deposition of different materials, such as 2D materials and single layers of complex oxide materials [26], with the potential to extend the concept of flexibility to emerging spintronic systems currently obtained on rigid substrates [30–33]. However, its compatibility with layered thin film heterostructures and industrial manufacturing processes has not yet been discussed. Ultra-thin Si wafers have high flexibility for thickness below 50 μm and are suitable for high-performance flexible electronics [28]; however, the thinning procedure applied to silicon substrates significantly complicates the overall process and raises the costs. As concerns the transfer-and-bonding approaches, two main strategies have been proposed [14,34–38]: i) *wet etching lift-off* approaches based on the selective solubility of sacrificial substrates/layers and ii) *dry transfer lift-off* methods exploiting the low adhesion strength between the rigid substrate and the layer system grown on top. The main advantages of these approaches are the possibility to use thermally stable crystalline and smooth substrates/layers, the compatibility with existing microfabrication processes and the possibility to transfer the structure on arbitrary flexible tapes. However, those methods are generally limited to small sizes.

In this work, we compare different strategies for the fabrication of flexible GMR spin-valves with PMA, including both transfer-and-bonding approaches and direct deposition on flexible substrates (Fig. 1**a-d**). The main characteristics, advantages, and drawbacks, as inferred from the data present in the literature, are summarized in Table 1. Concerning the direct deposition on flexible supports, inorganic MICA foils and Teonex® polymer tapes were used (Fig. 1**a**). Teonex® is a commercial PEN tape covered with a flattening coating (average surface roughness $R_a < 0.7$ nm) that offers high flexibility and a good heat stability (melting temperature $T_m \sim 525$ K) [25], which makes it suitable for the fabrication of complex thin film systems, provided that high processing and operating temperatures are not needed. As concerns the transfer-and-bonding approach, three different strategies were investigated exploiting i) water soluble crystalline salt substrates (i.e., KBr (1 0 0), Fig. 1**b**), ii) soluble polymer sacrificial underlayers (i.e., polymethylmethacrylate – PMMA, Fig. 1**c**) and low adhesion metal underlayers (i.e., Au on SiO_2/Si(1 0 0), Fig. 1**d**). Crystalline salt substrates and polymeric underlayers can be used to obtain flexible thin films by simple dissolution in water and polar solvents, respectively [36–38]. Differently to the PMMA sacrificial layer, which is amorphous and with a low melting temperature ($T_m \sim 435$ K), KBr (1 0 0) substrates supply a

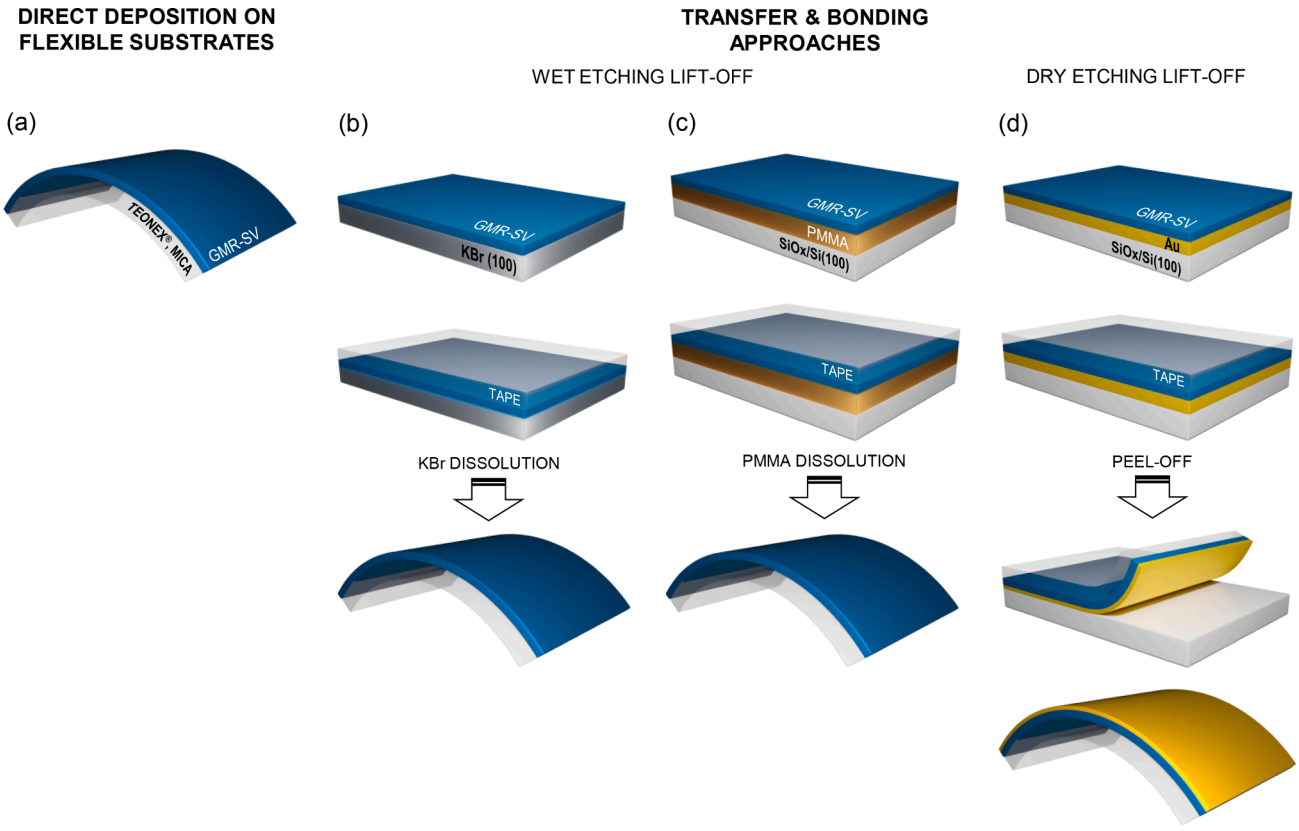

Fig. 1. Schematics of the different strategies explored to obtain flexible PMA GMR spin-valves. a) Direct deposition on flexible substrates, i.e., Teonex® tapes and freshly cleaved MICA foils. b, c) Transfer-and-bonding / Wet etching lift-off: b) freshly cleaved KBr (1 0 0) sheets and c) PMMA underlayers; after depositing the film stack, the whole structure is transferred on a flexible tape glued on top by dissolving KBr and PMMA in water and polar solvents, respectively. d) Transfer-and-bonding / Dry etching lift-off: Au underlayer; after depositing the film stack, the low adhesion between Au and SiOx/Si(1 0 0) is exploited to transfer the whole structure on a flexible tape glued on top by mechanical peel-off.

Table 1
Main advantages and drawbacks of selected strategies for the fabrication of flexible PMA GMR spin-valves.

	ADVANTAGES	DRAWBACKS
Direct deposition on flexible substrates		
Inorganic substratesFreshly cleaved MICA (muscovite) foils	· Crystalline and low-cost material · Atomically flat surface · One-step fabrication process · High processing and operating temperatures (up to ~800 K)	Low control of the cleavage process
Polymeric substrates Teonex® tapes - PEN films with a flattening coating (R_a < 0.7 nm)	· Low-cost material · One-step fabrication process · Large surface area coverage	· Amorphous coating · Low processing and operating temperatures ($T_{melting}$ ~ 525 K)
Transfer-and-bonding		
Wet etching lift-off		
Sacrificial salt substratesFreshly cleaved KBr (100) sheets	· Crystalline material · High processing temperatures ($T_{melting}$ ~ 1000 K) · Arbitrary flexible tapes can be used	· Costly substrates · Multi-step fabrication processes · Small surface area coverage
Sacrificial polymer underlayersPolymethylmethacrylate (PMMA)	· Low-cost material · Arbitrary flexible tapes can be used · Large surface area coverage	· Amorphous material · Multi-step fabrication processes · Low processing temperatures ($T_{melting}$ ~ 435 K)
Dry etching lift-off		
Low adhesion metal underlayersAu on SiOx/Si (100)	· Crystalline material · High processing temperatures · Arbitrary flexible tapes can be used	Multi-step fabrication processes

crystalline lattice that may affect the film growth and allows for high temperature processes (T_m ~ 1075 K). The low adhesion of metal layers (e.g., Cu, Ni, Au) on SiO_2 was already proposed as an efficient way to transfer thin films and heterostructures on flexible substrates by mechanical peel-off [14,34,35]. The feasibility of the direct deposition on Teonex® tapes and the Au-mediated transfer-and-bonding approach was already demonstrated by the authors of the present paper [14–16], and some data will be briefly recalled here to allow for a meaningful comparison with the other strategies.

Aiming at investigating the potential of the above mentioned strategies, [Co/Pd]-based thin film heterostructures, consisting of a fully compensated $[Co/Pd]_N/Ru/[Co/Pd]_N$ synthetic antiferromagnetic reference electrode (SAF-RL) and a $[Co/Pd]_N$ free-layer (FL) separated by a thin Cu spacer were used as model system. Co/Pd multilayers and their family members (e.g., Co/Pt and Co/Ni) are well known materials featured by a large interfacial PMA and tunable magnetic properties [39–42], which do not need high processing temperatures. SAF thin films stacks, consisting of two ferromagnetic layers separated by a thin metallic spacer were described for the first time in the 90 s of the last century [43] and since then have been widely investigated for many applications ranging from data storage/processing and sensor technologies [14,15,41,44–47] to biomedicine [48,49], being also of potential interest for other applications where single phase magnetic particles are commonly used [50–53]. SAF thin films are usually employed as reference electrode in GMR spin-valves and magnetically tunneling junctions [14–16,46,47], thanks to the strong and tunable antiferromagnetic coupling and to the zero-stray field at remanence [54,55]. The high complexity of Co/Pd-based spin-valves containing several interfaces whose quality strongly affects the overall properties (i.e., PMA of the Co/Pd multilayer, efficiency of the interlayer coupling in the SAF reference layer, GMR ratio) [56–59], makes the system a perfect candidate to test the effectiveness of the proposed strategies.

2. Experimental details

2.1. Materials and methods

PMA GMR spin-valves consisting of a $[Co(0.4)/Pd(0.9)]_3/Co(0.4)/Ru(0.4)/Co(0.4)/[Pd(0.9)/Co(0.4)]_3$ SAF reference electrode and a $[Co(0.4)/Pd(0.9)]_2$ free-layer (thicknesses in nanometers) separated by a 3 nm thick Cu spacer (Fig. 2) were deposited at room temperature by DC magnetron sputtering (BESTEC UHV system). Aiming at obtaining a strong PMA, a Ta(10)/Pd(3) seed layer was used to favor the growth of [Co/Pd] multilayers with a [111] texture [60,61]. A Pd(2.1) capping layer was deposited to prevent the free layer oxidation. Based on our previous works [14,15,49], the thickness of the individual layers and the number of the Co/Pd bilayer repetitions were selected to ensure i) a perpendicular magnetic anisotropy, ii) a strong antiferromagnetic coupling in the SAF structure and iii) two stable magnetization configurations (parallel/antiparallel) in the spin-valve systems. All the layers

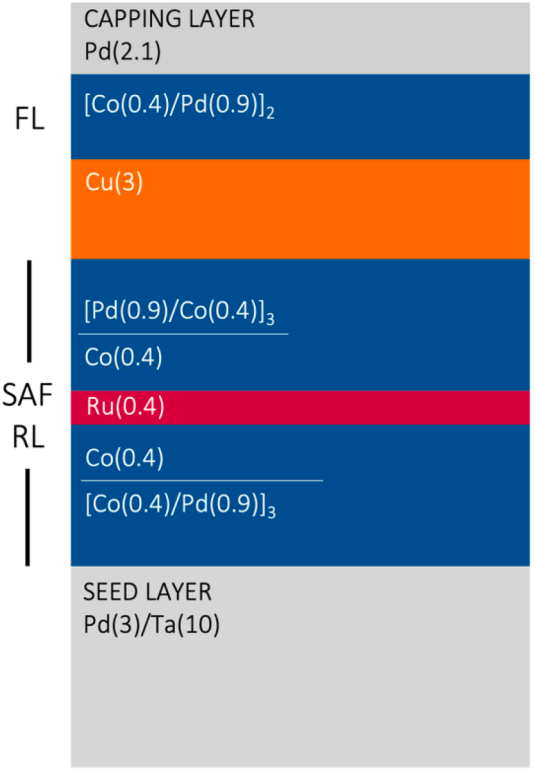

Fig. 2. Schematic structure of the Co/Pd-based GMR spin-valve stack consisting of a fully compensated $[Co/Pd]_3/Co/Ru/Co/[Pd/Co]_3$ synthetic antiferromagnet reference electrode (SAF-RL) and a $[Co/Pd]_2$ free-layer (FL) separated by a Cu spacer (thicknesses are given in nanometers).

were deposited under an Ar pressure of 3.5 μbar while the deposition rate was set to 0.067 nm/s (24 W-DC) for Au, 0.03 nm/s (40 W-DC) for Ta, 0.04 nm/s (26 W-DC) for Pd, 0.025 nm/s (52 W-DC) for Co, and 0.03 nm/s (48 W-DC) for Ru.

2.2. Fabrication of devices

Flexible spin-valves were fabricated by following the procedures reported below and schematically described in Fig. 1. For comparison, reference samples were also deposited on rigid SiOx/Si(1 0 0) substrates under the same experimental conditions.

- *Direct deposition on Teonex® polymer tapes*. Teonex® flexible tapes consisting of a 125 μm thick PEN film covered with a flattening coating (nominal surface roughness $R_a \approx 0.7$ nm) were purchased from *Teijin Corporation* and used as received.
- *Direct deposition on MICA substrates*. Flexible MICA foils were obtained by cleavage of natural muscovite (*Nilaco Corporation*) using a thin razor blade. Freshly cleaved MICA sheets were immediately introduced in the vacuum deposition chamber to minimize surface contamination.
- *Wet etching lift-off: KBr (1 0 0) sacrificial substrates*. KBr substrates were obtained by cleavage of KBr (1 0 0) single crystal cubes (*MSE Supplies*) using a thin razor blade. Freshly cleaved KBr substrates were immediately introduced in the vacuum deposition chamber to minimize surface contamination. After depositing the film stack, a Kapton adhesive tape was pasted to the sample surface and the whole structure was then immersed in deionized water to dissolve the KBr substrate.
- *Wet etching lift-off: PMMA sacrificial underlayers*. Polymethylmethacrylate (PMMA) sacrificial layers (thickness: 100 nm) were spin coated on thermally oxidized Si(1 0 0) substrates. After depositing the film stack, a Kapton adhesive tape was pasted to the sample surface and the whole structure was then immersed in acetone for a few seconds to dissolve the PMMA sacrificial layer only (Kapton is resistant to acetone). The SiOx/Si(1 0 0) rigid substrate was gently moved away using tweezers.
- *Dry etching lift-off: low adhesion Au metal underlayers*. 10 nm thick Au underlayers were deposited on SiOx/Si(1 0 0) substrates prior to the deposition of the thin film. Owing to the low adhesion between Au and SiOx, the film system was easily transferred on a commercial polyester tape (3 M 396) by mechanical peel-off. Details about the procedure are reported elsewhere [14].

2.3. Samples' characterization

Field-dependent magnetization loops were recorded at room temperature by using both superconductive interference device – vibrating sample magnetometry (SQUID-VSM, LOT-QuantumDesign, MPMS3) and VSM (Microsense, Model 10) with the magnetic field applied along the normal to the film plane.

The magneto-resistance (MR) was characterized at room temperature using the van der Pauw method. Four contacts were realized by silver paint at the corners of the sample and used to inject currents and measure the corresponding non-local voltage to determine the resistance of the heterostructure. Electrical currents in the order of 10 mA were injected in a current-in-plane geometry using a Keithley 6221 current source; non-local voltages were measured by a Keithley 2182A nanovoltmeter. Interchanging the current and voltage terminals, fundamental to average out asymmetries and inhomogeneities, was achieved by implementing an automated resistance measurement setup [62]. Sweeps in external magnetic field were performed using a standard dipole electromagnet (GMW Associates).

The analysis of the samples surface was performed by scanning electron microscopy (SEM) techniques using a Zeiss Supra 40 field-emission microscope. The samples were accurately attached on stubs and analysed without any preparation. Transmission electron microscopy (TEM) analysis was carried out by a Philips CM200 microscope operating at 200 kV and equipped with a LaB_6 filament. For observations, samples were prepared in cross-section by the conventional procedure consisting in the realization of a "sandwich", in the cutting of the slices, in the mechanical polishing with sandpapers, diamond pasts and a dimple-grinder machine. Final thinning was carried out by ion milling in a Gatan PIPS using 5 kV Ar^+ ions.

3. Results and discussion

3.1. Direct deposition on flexible substrates

Large area flexible spin-valves were obtained by direct deposition on Teonex® tapes and freshly cleaved MICA foils (inset of Fig. 3**a,b and 3c, d**, respectively). The corresponding room temperature field-dependent magnetization loops recorded with the field applied along the film normal are reported in Fig. 3**a and 3c.** In both cases, the loops show a characteristic three-step magnetization response associated to the individual sharp reversals of the bottom/top layers of the reference electrode and the free-layer of the spin-valve. No significant differences are observed with respect to the reference samples deposited on a SiOx/Si (1 0 0) rigid substrate (Fig. S1**a**, Supplementary Information), except for minor changes in the coercivity and reverse field of the individual layers (**Table S2** in the Supplementary Information) that may be associated to the specific surface morphology and roughness of the different substrates. A very smooth surface is observed for thin film systems deposited on Teonex® (Fig. 3**e**). However, the slightly higher surface roughness of Teonex® ($R_a \approx 0.7$ nm) as compared to the SiOx/Si (1 0 0) substrates (0.2 – 0.3 nm) [49] would lead to a slight increase in the interface roughness (Fig. 3**g**), resulting in some inhomogeneity, defects, and modified interlayer interactions, which may lead to minor effects on the final magnetic properties. On the other hand, freshly cleaved MICA foils consist of extended, micrometer-sized, and atomic flat terraces (inset of Fig. 3**f**), which should lead to very smooth thin film interfaces (Fig. 3**h**). While the magnetic behavior of the spin-valves on Teonex® and MICA are very similar, the magneto-resistive (MR) properties are rather different as evident in Fig. 3**b and 3d**, respectively. The flexible GMR-SV on Teonex® shows the typical behavior expected for a PMA spin-valve with a SAF reference layer (Fig. 3**b**), similar to the reference sample (Fig. S1**b**, Supplementary Information). Starting from saturation, the relative resistance change [$\Delta R/R_{low} = (R_{high} - R_{low})/R_{low}$] shows a steep increase in correspondence of the switch of the SAF top layer, which determines an antiparallel configuration of the magnetization across the Cu spacer, and then reduces to a lower value when the FL switches (parallel configuration). A further increase of the reverse field leads to an additional reduction of the resistance when the magnetization of the SAF bottom layer is also aligned along the external field. The spin-valve shows a maximum GMR ratio of ~3.4 ± 0.2 % that is close to the value measured in the reference sample (~4.5 ± 0.3 %). Flexible spin-valves on cleaved MICA foils show a comparable GMR ratio (3.2–3.6 %), thus confirming the high quality of the film stack. However, the electrical response is not fully reproducible (**Figure S3** in the Supplementary Information) and a different behavior is observed when the external field is swept from positive to negative values and vice-versa (Fig. 3**d**). This indicates a non-symmetric magnetization switching of the bottom and top layers of the SAF versus field sweeping direction, as schematically reported in the sketches of Fig. 3**c**. Starting from the negative saturation state (ascending branch, red curve), the bottom SAF layer reverses first; on the contrary, when the external field moves from positive to negative values (descending branch, light blue curve), the reversal starts in the top SAF layer thus determining a high electrical resistance state resulting from the antiparallel configuration of the magnetization of the two layers at the Cu interface. Together with the experimental evidence that the magneto-electrical behaviour differs from sample to sample and for different paths of the probing current within the same sample (refer to

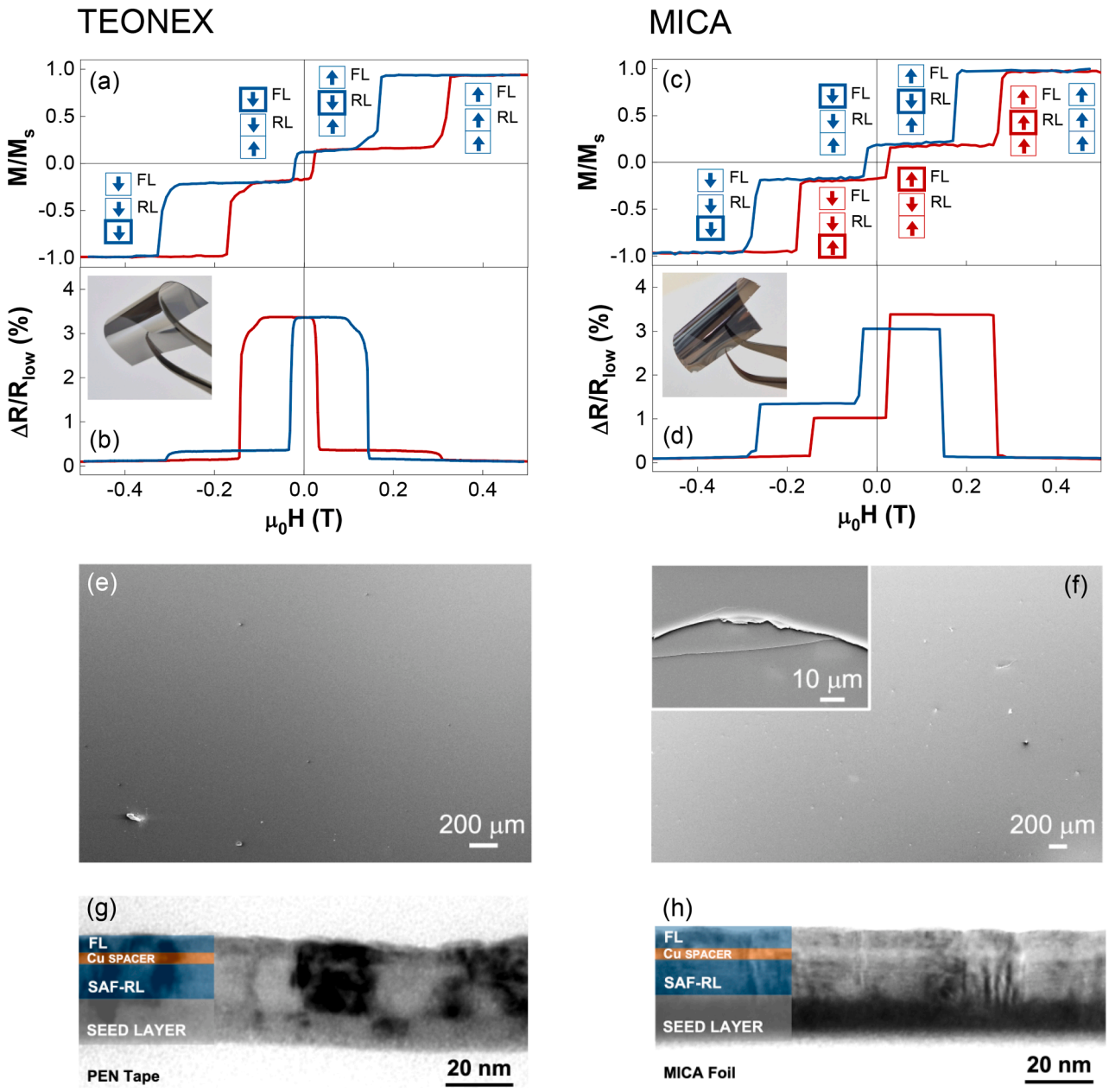

Fig. 3. Flexible Co/Pd-based PMA GMR-SVs prepared by direct deposition on (left column) Teonex® polymer tapes and (right column) freshly cleaved MICA foils. Room temperature (a,c) out-of-plane magnetization loops normalized to the saturation magnetization $M/M_s(H)$, and corresponding (b,d) $\Delta R/R_{low} = (R_{high} - R_{low})/R_{low}$ magnetoresistive curves. Different colors are used to represent magnetic field sweeps from positive to negative (in light blue, descending curve) and from negative to positive (in red, ascending curve) with respect to the surface normal. The sketch of the heterostructure with the arrows denotes the evolution of the magnetization in the free-layer (FL) and the bottom/top layers of the reference electrode (RL) as a function of the external magnetic field; the thick boxes indicate which layer reverses after each critical step in the hysteresis loop. Owing to the asymmetrical reversal in the samples deposited on MICA foils, panel c reports the schematics of the evolution of the magnetization for both the upward and downward branches determined from the MR curve. Inset: optical photographs of flexible structures. (e, f) SEM plan view and (g, h) TEM cross sections of samples deposited on (e, g) Teonex® and (f, h) MICA, respectively. (For interpretation of the references to colour in this figure legend, the reader is referred to the web version of this article.)

Figure S3 in the Supplementary Information for comparison), we conclude that the two magnetic configurations of the SAF reference electrode have comparable energies and slight variations possibly determine the observed variability and asymmetry. The origin of the peculiar behavior of MR curves of spin-valves deposited on MICA sheets is not fully disclosed, although we believe it is related to the hardly controllable morphology of the cleaved MICA surface consisting of micrometer-sized atomic flat terraces. We suppose that such terraces are large and thick enough that they do not induce major effects at the level of the single interfaces in the film stack, and on the overall magnetic properties, as well. However, the presence of defective steps between terraces can possibly affect the nucleation and propagation of magnetic domains, as well as the local electric properties, thus leading to slight changes in the magneto-transport properties due to the randomness of the step formation during the peeling process.

The results indicate that MICA foils could have potential for high-quality magnetic heterostructures, although their morphology (e.g., the presence of steps) does not allow a reproducible electrical behavior at the present stage. On the contrary, Teonex® is highly suitable for obtaining high-quality GMR-SVs provided that high processing and

operating temperatures are not required.

3.2. Transfer-and-bonding strategies

All the lift-off strategies here explored allowed transferring the film stack on a flexible tape (insets of Fig. 4**b, 4f and 4m**). However, clear differences were observed and not all the approaches are suitable to obtain high-quality flexible PMA SVs.

On freshly cleaved KBr (100) substrates, the typical three-steps magnetization reversal is hardly observed both before and after substrate dissolution and transferring of the film stack on Kapton (Fig. 4**a and 4b**, respectively), suggesting the absence of smooth surface/interfaces. Large area SEM images of the surface of freshly cleaved KBr substrates and SVs before the lift-off process (Fig. 4**c**) shows that the surface of the KBr substrate is characterized by the presence of many cleavage steps (Fig. 4**c** left) that induce inhomogeneity and layer intermixing inside the deposited thin film, as suggested by the presence of line defects on the film surface (Fig. 4**c** right). Such defects are supposed to be responsible for the open circuit electric behavior of the stack on micrometric distances, which in turn prevents any magneto-resistive measurements.

In contrast, reasonable magnetic and transport properties are obtained by using a PMMA sacrificial underlayer (Fig. 4**d and 4e**). With respect to the rigid counterpart, we detected a slight increase of the coercivity for the SAF bottom and top layers (**Table S2** in the Supplementary Information), and a lower GMR ratio (~2 %), likely due to defects and inhomogeneities induced by the higher surface roughness of PMMA (typically of the order of few nanometers [63]). An improvement of the magnetic and transport properties may be provided by a further optimization of the PMMA resist process, for example by a thermal reflow usually used to generate ultra-smooth optical surfaces [64]. Upon transferring of the thin film on an adhesive Kapton tape, the magnetic behavior remains unchanged (Fig. 4**f**), although a high electrical resistance was detected, preventing magneto-resistive measurements.

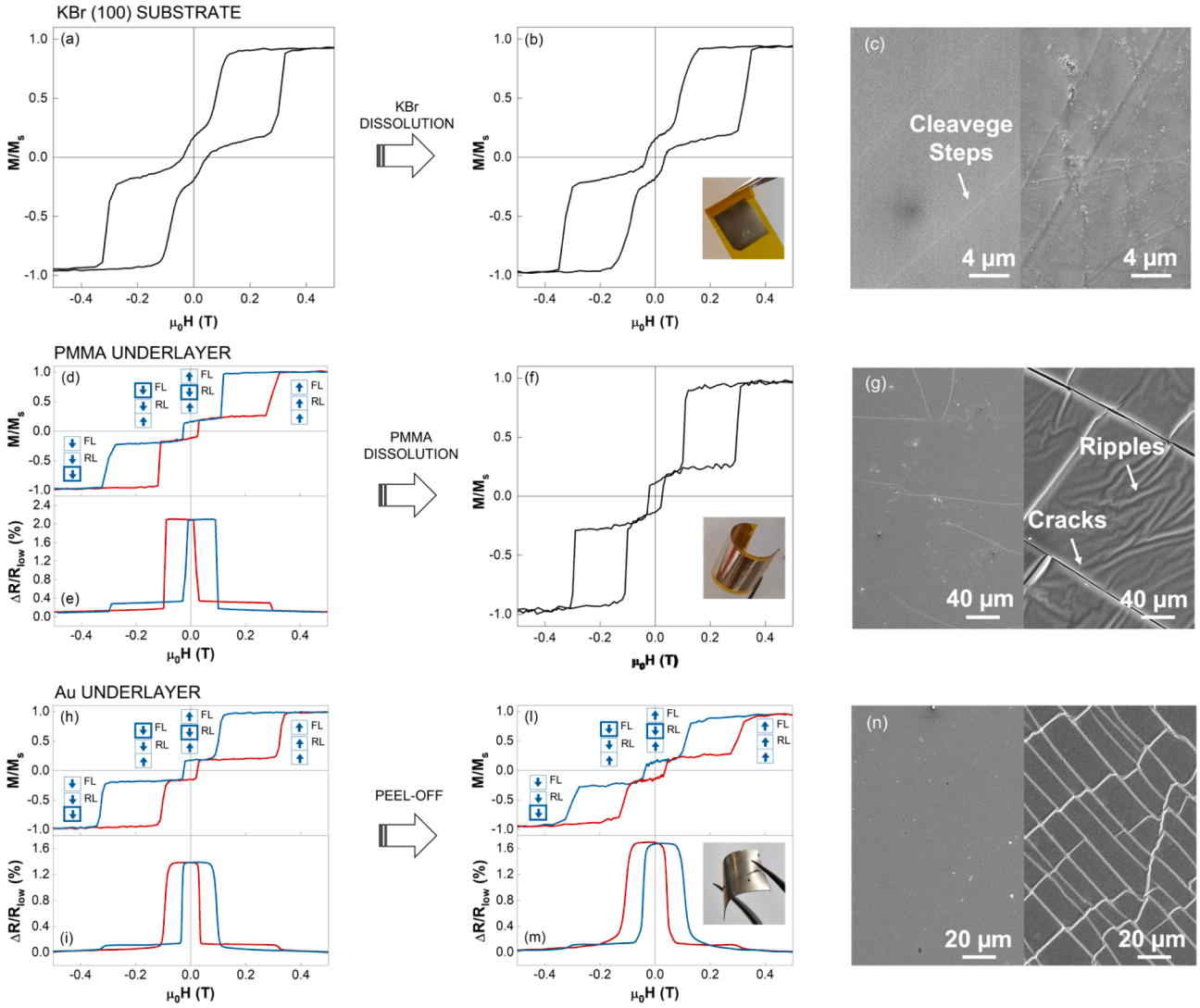

Fig. 4. Flexible Co/Pd-based PMA GMR-SVs obtained by transfer-and-bonding approaches: (top panel) KBr (100) sacrificial substrate, (middle panel) PMMA sacrificial underlayer, (bottom panel) low-adhesion Au underlayer. (a, b, d, f, h, l) Room temperature out-of-plane magnetization loops normalized to the saturation magnetization, $M/M_s(H)$, and (e, i, m) corresponding $\Delta R/R_{low} = (R_{high} - R_{low})/R_{low}$ magneto-resistive curves: (left figure) before and (middle figures) after the lift-off process. Where present, to better visualize the electrical response and its relationship with the M(H) loop, different colors are used for the descending (light blue) and ascending (red) branches. The arrows indicate the evolution of the magnetization in the free-layer (FL) and bottom/top layers of the reference electrode (RL) as a function of the external magnetic field; the thick boxes indicate which layer reverses after each step in the hysteresis loop. Insets: optical photographs of flexible structures. (c) SEM plan view of the KBr (1 0 0) surface (left) and the GMR-SV deposited on top before peeling (right). (g, n) SEM plan view of the surface before (left) and after (right) the lift-off process of samples obtained by using a (g) PMMA sacrificial underlayer and a (n) Au low-adhesion layer, respectively. (For interpretation of the references to colour in this figure legend, the reader is referred to the web version of this article.)

Indeed, SEM images indicate that the magnetic film has a uniform structure on PMMA (Fig. 4**g** left), while the lift-off process is responsible for the formation of many cracks (Fig. 4**g** right). Moreover, there are clear ripples among the cracks, possibly caused by the evaporation of the glue in the adhesive Kapton tape in the vacuum of the microscope. The results indicate that PMMA is a good sacrificial layer although the release process requires further improvements to optimize the transfer of the films on the flexible tape.

Finally, large area and fully working flexible SVs can be obtained by exploiting the low adhesion of Au underlayers on SiOx/Si(1 0 0) substrates. The magnetic and transport properties remain basically unchanged after the lift-off process (Fig. 4**h,i** and **4l,m**) and just minor differences with respect to the reference sample (**Table S2** in the Supplementary Information) are observed owing to the higher roughness of the Au underlayer (as evidenced by TEM analysis presented in **Figure S4** of the Supplementary Information). SEM analysis reveals a uniform structure in both cases (Fig. 4**n**). The white intersecting lines visible on the surface of the flexible SVs, indicate the presence of local swellings due to the evaporation of the glue inside the vacuum chamber of the microscope, as previously assumed, or to the peeling process it-self. However, without major impact on the overall magneto-transport properties. These findings indicate the feasibility of such a method to obtain complex spintronic thin film systems, with the potential to be also exploited for systems requiring high processing temperatures.

4. Conclusions and perspectives

Different strategies to realize flexible PMA SVs with their specific features have been investigated and compared. They include i) the direct deposition on two different flexible substrates, i.e., Teonex® polymer tapes and freshly cleaved inorganic MICA foils, and ii) transfer-and-bonding approaches exploiting wet lift-off methods based on sacrificial substrates/layers soluble in water and polar solvents as well as dry lift-off process exploiting the low adhesion of Au metal underlayers on SiOx/Si(1 0 0) substrates. [Co/Pd]-based GMR-SVs (with a synthetic antiferromagnet as a reference layer) were used as test case, as the high complexity of the layer stacks in terms of number of interfaces allows to get insights on the quality of those interfaces that are affected by the fabrication process.

Direct deposition of GMR-SVs on flexible substrates. Teonex® tapes are the best choice to obtain high-quality spintronic thin films on large area, provided that relatively low processing and operating temperatures (<525 K) are required. MICA foils are instead suitable for high temperature processing and potentially attractive for their atomically flat large terraces. However, the presence of steps that possibly induces local modifications of the magnetic and electrical properties that randomly influence the magneto-electric response, makes such substrates unsuitable for these applications, unless a method to obtain foils free of terraces is developed.

Transfer-and-bonding strategies. A sacrificial underlayer of PMMA is very attractive for the limited cost of the solution. However, the experimental evidence underlined some difficulties and further investigations are necessary to improve the release process and the transfer of complex spintronic thin film systems on flexible tapes. This would require, for example, a proper functionalization of the film surface to allow for a stronger and homogeneous bond to the tape surface. The same holds for the use of sacrificial salt substrates, such as water-soluble KBr, which present many cleavage steps that limit their effectiveness. This issue may be addressed by using KBr underlayers with a controlled surface roughness deposited just before the growth of the thin film structure. On the other hand, the use of a low adhesion Au underlayer has proven to be very effective for the fabrication of complex spintronic thin film systems on large area flexible substrates, with the potential to be also exploited for systems requiring high processing temperatures.

The present work provides an overview of possible approaches to flexible spintronics, highlighting the strengths and weaknesses of some approaches and providing a pathway for the development of flexible spintronic devices with a complex architecture.

CRediT authorship contribution statement

Mariam Hassan: Investigation, Formal analysis. **Sara Laureti:** Formal analysis. **Christian Rinaldi:** Formal analysis, Writing – review & editing. **Federico Fagiani:** Investigation, Formal analysis. **Gianni Barucca:** Investigation, Formal analysis. **Annamaria Gerardino:** Investigation. **Nataliia Schmidt:** Investigation. **Mario Fix:** Investigation. **Manfred Albrecht:** Conceptualization, Writing – review & editing. **Gaspare Varvaro:** Conceptualization, Supervision, Writing – original draft.

Declaration of Competing Interest

The authors declare that they have no known competing financial interests or personal relationships that could have appeared to influence the work reported in this paper.

Data availability

Data will be made available on request.

Acknowledgments

G.V. and S.L. acknowledges the technical support provided by Enrico Patrizi for the magnetic characterization of the samples. C.R. and F.F. acknowledge Polifab, the micro and nanofabrication facility of Politecnico di Milano, for supporting the investigation of transport properties. C.R. acknowledges the support from the Italian Ministry Research (MUR) under the PRIN program, project No. 2017YCTB59 (TWEET. ToWards fErroElectricity in Two-dimensions).

Appendix A. Supplementary data

Supplementary data to this article can be found online at https://doi.org/10.1016/j.apsusc.2023.157740.

References

[1] B. Dieny, M. Chshiev, Perpendicular magnetic anisotropy at transition metal/oxide interfaces and applications, Rev. Mod. Phys. 89 (2017), https://doi.org/10.1103/RevModPhys.89.025008.
[2] V.K. Joshi, Spintronics: A contemporary review of emerging electronics devices, Eng. Sci. Technol. Int. J. 19 (2016) 1503–1513, https://doi.org/10.1016/j.jestch.2016.05.002.
[3] M.N. Baibich, J.M. Broto, A. Fert, F.N. Van Dau, F. Petroff, P. Eitenne, G. Creuzet, A. Friederich, J. Chazelas, Giant magnetoresistance of (001)Fe/(001)Cr magnetic superlattices, Phys. Rev. Lett. 61 (1988) 2472–2475, https://doi.org/10.1103/PhysRevLett.61.2472.
[4] G. Binasch, P. Grünberg, F. Saurenbach, W. Zinn, Enhanced magnetoresistance in layered magnetic structures with antiferromagnetic interlayer exchange, Phys. Rev. B 39 (1989) 4828–4830, https://doi.org/10.1103/PhysRevB.39.4828.
[5] M. Melzer, D. Makarov, A review on stretchable magnetic field sensorics, J. Phys. D Appl. Phys. Top. 53 (2020), 083002 (1–34).
[6] D. Makarov, M. Melzer, D. Karnaushenko, O.G. Schmidt, Shapeable magnetoelectronics, Appl. Phys. Rev. 3 (2016), https://doi.org/10.1063/1.4938497, 011101 (1–24).
[7] P. Sheng, B. Wang, R. Li, Flexible magnetic thin films and devices, J. Semicond. 39 (2018), https://doi.org/10.1088/1674-4926/39/1/011006, 011006 (1–13).
[8] G.S.C. Bermúdez, H. Fuchs, L. Bischoff, J. Fassbender, D. Makarov, Electronic-skin compasses for geomagnetic field-driven artificial magnetoreception and interactive electronics, Nat. Electron. 1 (2018) 589–595.
[9] G.S.C. Bermúdez, D.D. Karnaushenko, D. Karnaushenko, A. Lebanov, L. Bischoff, M. Kaltenbrunner, J. Fassbender, O.G. Schmidt, D. Makarov, Magnetosensitive e-skins with directional perception for augmented reality, Sci. Adv. 4 (2018), 2623 (1–9).
[10] S. Amara, G.A.T. Sevilla, M. Hawsawi, Y. Mashraei, H. Mohammed, M.E. Cruz, Y. P. Ivanov, S. Jaiswal, G. Jakob, M. Kläui, M. Hussain, J. Kosel, High-Performance Flexible Magnetic Tunnel Junctions for Smart Miniaturized Instruments, Adv. Eng. Mater. 20 (2018) 1800471–1800479, https://doi.org/10.1002/adem.201800471.

[11] J.Y. Chen, Y.C. Lau, J.M.D. Coey, M. Li, J.P. Wang, High performance MgO-barrier magnetic tunnel junctions for flexible and wearable spintronic applications, Sci. Rep. 7 (2017) 42001, https://doi.org/10.1038/srep42001.

[12] M. Melzer, M. Kaltenbrunner, D. Makarov, D. Karnaushenko, D. Karnaushenko, T. Sekitani, T. Someya, O.G. Schmidt, Imperceptible magnetoelectronics, Nat. Commun. 6 (2015), https://doi.org/10.1038/ncomms7080, 6080 (1–8).

[13] A. Bedoya-Pinto, M. Donolato, M. Gobbi, L.E. Hueso, P. Vavassori, Flexible spintronic devices on Kapton, Appl. Phys. Lett. 104 (2016), 062412, https://doi.org/10.1063/1.4865201.

[14] M. Hassan, S. Laureti, C. Rinaldi, F. Fagiani, S. Varotto, G. Barucca, N.Y. Schmidt, G. Varvaro, M. Albrecht, Perpendicularly magnetized Co/Pd-based magneto-resistive heterostructures on flexible substrates, Nanoscale Adv. 3 (2021) 3076–3084, https://doi.org/10.1039/d1na00110h.

[15] P. Makushko, E.S. Oliveros Mata, G.S. Cañón Bermúdez, M. Hassan, S. Laureti, C. Rinaldi, F. Fagiani, G. Barucca, N. Schmidt, Y. Zabila, T. Kosub, R. Illing, O. Volkov, I. Vladymyrskyi, J. Fassbender, M. Albrecht, G. Varvaro, D. Makarov, Flexible Magnetoreceptor with Tunable Intrinsic Logic for On-Skin Touchless Human-Machine Interfaces, Adv. Funct. Mater. 31 (2021), https://doi.org/10.1002/adfm.202101089, 2101089 (1–8).

[16] M. Hassan, S. Laureti, C. Rinaldi, F. Fagiani, G. Barucca, F. Casoli, A. Mezzi, E. Bolli, S. Kaciulis, M. Fix, A. Ullrich, Thin-Film Heterostructures Based on Co/Ni Synthetic Antiferromagnets on Polymer Tapes: Toward Sustainable Flexible Spintronics, ACS Appl Mater Interfaces 14 (45) (2022) 51496–51509, https://doi.org/10.1021/acsami.2c14000.

[17] H. Matsumoto, S. Ota, T. Koyama, D. Chiba, Biaxial strain sensing using a Pd/Co-based perpendicular flexible spin valve, Appl. Phys. Express. 15 (2022) 033004, https://doi.org/10.35848/1882-0786/ac5725.

[18] S. Mohanty, M. Sharma, A.K. Moharana, B. Ojha, E. Pandey, B.B. Singh, S. Bedanta, Magnetization Reversal and Domain Structures in Perpendicular Synthetic Antiferromagnets Prepared on Rigid and Flexible Substrates, Jom 74 (2022) 2319–2327, https://doi.org/10.1007/s11837-022-05300-5.

[19] S. Eimer, H. Cheng, J. Li, X. Zhang, C. Zhao, W. Zhao, Perpendicular magnetic anisotropy based spintronics devices in Pt/Co stacks under different hard and flexible substrates, Sci. China Inf. Sci. 66 (2023), 122408, https://doi.org/10.1007/s11432-021-3371-4.

[20] R. Bertacco, M. Cantoni, New trends in magnetic memories, in: G. Varvaro, F. Casoli (Eds.), Ultra-High Density Magn. Rec. Mater., Pan Stanford Publishing, 2016.

[21] S. Bhatti, R. Sbiaa, A. Hirohata, H. Ohno, S. Fukami, S.N. Piramanayagam, Spintronics based random access memory : a review, Mater. Today 20 (2017) 530–548, https://doi.org/10.1016/j.mattod.2017.07.007.

[22] J. Ryu, S. Lee, K. Lee, B. Park, Current-Induced Spin – Orbit Torques for Spintronic Applications, Adv. Mater. 32 (2020) 1907148, https://doi.org/10.1002/adma.201907148.

[23] W.S. Wong, A. Salleo, eds., Flexible Electronics: Materials and Applications, Springer, 2009. https://doi.org/10.1007/978-0-387-74363-9_4.

[24] W. Liu, H. Wang, Flexible oxide epitaxial thin films for wearable electronics: Fabrication, physical properties, and applications, J. Mater. 6 (2020) 385–396, https://doi.org/10.1016/j.jmat.2019.12.006.

[25] W.A. MacDonald, M.K. Looney, D. MacKerron, R. Eveson, R. Adam, K. Hashimoto, K. Rakos, Latest advances in substrates for flexible electronics, J. Soc. Inf. Disp. 15 (2007) 1075–1083, https://doi.org/10.1889/1.2825093.

[26] G. Zhong, J. Li, Muscovite mica as a universal platform for flexible electronics, J. Mater. 6 (2020) 455–457, https://doi.org/10.1016/j.jmat.2019.12.004.

[27] Y. Chu, Van der Waals oxide heteroepitaxy, Npj Quantum Mater. 2 (2017) 67, https://doi.org/10.1038/s41535-017-0069-9.

[28] S. Gupta, W.T. Navaraj, L. Lorenzelli, R. Dahiya, Ultra-thin chips for high-performance flexible electronics, Npj Flex. Electron. 2 (2018) 8, https://doi.org/10.1038/s41528-018-0021-5.

[29] S.M. Fortier, B.J. Giletti, Volume self-diffusion of oxygen in biotite, muscovite, and phlogopite micas, Geochim. Cosmochim. Acta. 55 (1991) 1319–1330, https://doi.org/10.1016/0016-7037(91)90310-2.

[30] M.F. Khan, S. Rehman, M.A. Rehman, M.A. Basit, D.K. Kim, F. Ahmed, H.W. Khalil, I. Akhtar, S.C. Jun, Modulation of Magnetoresistance Polarity in BLG/SL-$MoSe_2$ Heterostacks, Nanoscale Res. Lett. 15 (2020) 1–18, https://doi.org/10.1186/s11671-020-03365-2.

[31] P.U. Asshoff, J.L. Sambricio, A.P. Rooney, S. Slizovskiy, A. Mishchenko, A. M. Rakowski, E.W. Hill, A.K. Geim, S.J. Haigh, V.I. Fal'Ko, I.J. Vera-Marun, Magnetoresistance of vertical Co-graphene-NiFe junctions controlled by charge transfer and proximity-induced spin splitting in graphene, 2D Mater. 4 (2017), 031004, https://doi.org/10.1088/2053-1583/aa7452.

[32] M.F. Khan, S. Rehman, M.A. Rehman, R.U. Rehman Sagar, D.K. Kim, H.M. Waseem Khalil, P.A. Shinde, P.R. Sharma, J. Eom, S. Chan Jun, Multi-heterostructured spin-valve junction of vertical FLG/$MoSe_2$/FLG, APL Mater. 8 (2020), 071104, https://doi.org/10.1063/5.0006267.

[33] Q. Wang, Y. Gu, C. Chen, F. Pan, C. Song, Oxide Spintronics as a Knot of Physics and Chemistry: Recent Progress and Opportunities, J. Phys. Chem. Lett. 13 (2022) 10065–10075, https://doi.org/10.1021/acs.jpclett.2c02634.

[34] C.H. Lee, J. Kim, C. Zou, I.S. Cho, J.M. Weisse, W. Nemeth, Q. Wang, A.C.T. Van Duin, T. Kim, X. Zheng, Peel-and-Stick: mechanism study for efficient fabrication of flexible/transparent thin-film electronics, Sci. Rep. 3 (2013), https://doi.org/10.1038/srep02917, 2917 (1–6).

[35] M. Donolato, C. Tollan, J.M. Porro, A. Berger, P. Vavassori, Flexible and Stretchable Polymers with Embedded Magnetic Nanostructures, Adv. Mater. 25 (2013) 623–629, https://doi.org/10.1002/adma.201203072.

[36] F. An, K. Qu, G. Zhong, Y. Dong, W. Ming, M. Zi, Z. Liu, Y. Wang, B. Qi, Z. Ding, J. Xu, Z. Luo, X. Gao, S. Xie, P. Gao, J. Li, Highly Flexible and Twistable Freestanding Single Crystalline Magnetite Film with Robust Magnetism, 2003495 (1–7), Adv. Funct. Mater. 30 (2020), https://doi.org/10.1002/adfm.202003495.

[37] D.K. Lee, S. Kim, S. Oh, J.Y. Choi, J.L. Lee, H.K. Yu, Water-Soluble Epitaxial NaCl Thin Film for Fabrication of Flexible Devices, Sci. Rep. 7 (2017), https://doi.org/10.1038/s41598-017-09603-5, 8716 (1–7).

[38] M. Melzer, D. Karnaushenko, G. Lin, S. Baunack, D. Makarov, O.G. Schmidt, Direct transfer of magnetic sensor devices to elastomeric supports for stretchable electronics, Adv. Mater. 27 (2015) 1333–1338, https://doi.org/10.1002/adma.201403998.

[39] M.T. Johnson, P.J.H. Bloemen, F.J.A. den Broeder, J.J. de Vries, Magnetic anisotropy in metallic multilayers, Rep. Prog. Phys. 59 (1996) 1409–1458, https://doi.org/10.1088/0034-4885/59/11/002.

[40] A. Verna, P. Alippi, F. Offi, G. Barucca, G. Varvaro, E. Agostinelli, M. Albrecht, B. Rutkowski, A. Ruocco, D. Paoloni, M. Valvidares, S. Laureti, Disclosing the Nature of Asymmetric Interface Magnetism in Co/Pt Multilayers, ACS Appl. Mater. Interfaces 14 (2022) 12766–12776, https://doi.org/10.1021/acsami.1c22341.

[41] M. Arora, N.R. Lee-Hone, T. Mckinnon, C. Coutts, R. Hübner, B. Heinrich, D. M. Broun, E. Girt, Magnetic properties of Co / Ni multilayer structures for use in STT-RAM, J. Phys. D Appl. Phys. 50 (2017), 505003.

[42] O. Hellwig, T. Hauet, T. Thomson, E. Dobisz, J.D. Risner-Jamtgaard, D. Yaney, B. D. Terris, E.E. Fullerton, Coercivity tuning in Co/Pd multilayer based bit patterned media, Appl. Phys. Lett. 95 (2009), https://doi.org/10.1063/1.3271679, 232505 (3 pp).

[43] S.S.P. Parkin, Systematic Variation of the Strength and Oscillation Period of Indirect Magnetic Exchange Coupling through the 3d, 4d, and Sd Transition Metals, Phys. Rev. Lett. 67 (1991) 3598–3601.

[44] W. Legrand, D. Maccariello, F. Ajejas, S. Collin, A. Vecchiola, K. Bouzehouane, N. Reyren, V. Cros, A. Fert, Room-temperature stabilization of antiferromagnetic skyrmions in synthetic antiferromagnets, Nat. Mater. 19 (2020) 34–42, https://doi.org/10.1038/s41563-019-0468-3.

[45] X. Wang, Q. Yang, L. Wang, Z. Zhou, T. Min, M. Liu, N.X. Sun, E-field Control of the RKKY Interaction in FeCoB/Ru/FeCoB/PMN-PT (011) Multiferroic Heterostructures, Adv. Mater. 30 (2018) 1803612, https://doi.org/10.1002/adma.201803612.

[46] K. Yakushiji, H. Kubota, A. Fukushima, S. Yuasa, Perpendicular magnetic tunnel junctions with strong antiferromagnetic interlayer exchange coupling at first oscillation peak, Appl. Phys. Express. 8 (2015), 083003, https://doi.org/10.7567/APEX.8.083003.

[47] Y. Chang, V. Garcia-vazquez, Y. Chang, T. Wu, Perpendicular magnetic tunnel junctions with synthetic antiferromagnetic pinned layers based on [Co/Pd] multilayers, J. Appl. Phys. 113 (2016) 17B909, https://doi.org/10.1063/1.4799974.

[48] E.N. Welbourne, T. Vemulkar, R.P. Cowburn, High-yield fabrication of perpendicularly magnetised synthetic antiferromagnetic nanodiscs, Nano Res. 14 (2021) 3873–3878, https://doi.org/10.1007/s12274-021-3307-1.

[49] G. Varvaro, S. Laureti, D. Peddis, M. Hassan, G. Barucca, P. Mengucci, A. Gerardino, E. Giovine, O. Lik, D. Nissen, M. Albrecht, Co/Pd-Based synthetic antiferromagnetic thin films on Au/resist underlayers: Towards biomedical applications, Nanoscale 11 (2019) 21891–21899, https://doi.org/10.1039/c9nr06866j.

[50] D. Peddis, S. Laureti, D. Fiorani (Eds.), New trends in nanoparticles magnetism, 2021st ed., Springer, Berlin Heidelberg, 2018.

[51] Z. Ma, J. Mohapatra, K. Wei, J.P. Liu, S. Sun, Magnetic Nanoparticles: Synthesis, Anisotropy, and Applications, Chem. Rev. (2021), https://doi.org/10.1021/acs.chemrev.1c00860.

[52] P.P. Falciglia, E. Gagliano, P. Scandura, C. Bianco, T. Tosco, R. Sethi, G. Varvaro, E. Agostinelli, C. Bongiorno, A. Russo, S. Romano, G. Malandrino, P. Roccaro, F.G. A. Vagliasindi, Physico-magnetic properties and dynamics of magnetite (Fe_3O_4) nanoparticles (MNPs) under the effect of permanent magnetic fields in contaminated water treatment applications, Sep. Purif. Technol. 296 (2022), 121342, https://doi.org/10.1016/j.seppur.2022.121342.

[53] C. Scialabba, R. Puleio, D. Peddis, G. Varvaro, P. Calandra, G. Cassata, L. Cicero, M. Licciardi, G. Giammona, Folate targeted coated SPIONs as efficient tool for MRI, Nano Res. 10 (2017) 3212–3227, https://doi.org/10.1007/s12274-017-1540-4.

[54] S. Bandiera, R.C. Sousa, Y. Dahmane, C. Ducruet, C. Portemont, V. Baltz, S. Auffret, I.L. Prejbeanu, B. Dieny, Comparison of Synthetic Antiferromagnets and Hard Ferromagnets as Reference Layer in Magnetic Tunnel Junctions With Perpendicular Magnetic Anisotropy, IEEE Magn. Lett. 1 (2010) 3000204.

[55] J.A. Katine, E.E. Fullerton, Device implications of spin-transfer torques, J. Magn. Magn. Mater. 320 (2008) 1217–1226, https://doi.org/10.1016/j.jmmm.2007.12.013.

[56] J. Qiu, Z. Meng, Y. Yang, J.F. Ying, Q.J. Yap, G. Han, Effect of roughness on perpendicular magnetic anisotropy in (Co90Fe10/Pt)n superlattices, AIP Adv. 6 (2016), https://doi.org/10.1063/1.4944520, 056123 (1–5).

[57] A. Paul, Effect of interface roughness on magnetic multilayers of Fe/Tb and Fe/Cr, J. Magn. Magn. Mater. 240 (2017) 497–500, https://doi.org/10.1016/S0304-8853(01)00912-X.

[58] M. Desai, A. Misra, W.D. Doyle, Effect of Interface Roughness on Exchange Coupling in Synthetic Antiferromagnetic Multilayers, IEEE Trans. Magn. 41 (2005) 3151–3153.

[59] E.Y. Tsymbal, D.G. Pettifor, Perspectives of Giant Magnetoresistance, in: H. Ehrenreich, F. Spaepen (Eds.), Solid State Phys, Vol 56, Academic, New York, 2001, pp. 113–237.

[60] F.J.A. Den Broeder, D. Kuiper, H.C. Donkersloot, W. Hoving, A comparison of the magnetic anisotropy of [001] and [111] oriented Co/Pd Multilayers, Appl. Phys. A. 49 (1989) 507–512, https://doi.org/10.1007/BF00617017.
[61] K. Tobari, M. Ohtake, K. Nagano, M. Futamoto, Preparation and characterization of Co/Pd epitaxial multilayer films with different orientations, Jpn. J. Appl. Phys. 50 (2011), https://doi.org/10.1143/JJAP.50.073001.
[62] S.K. Pandey, A. Manivannan, A fully automated temperature-dependent resistance measurement setup using van der Pauw method, Rev. Sci. Instrum. 89 (2018) 33906.
[63] PMMA datasheet, (n.d.). https://www.allresist.com/wp-content/uploads/sites/2/2021/05/Allresist_Product-information-E-beamresist-English-web.pdf.
[64] R. Kirchner, H. Schift, Thermal reflow of polymers for innovative and smart 3D structures: A review, Mater. Sci. Semicond. Process. 92 (2019) 58–72, https://doi.org/10.1016/j.mssp.2018.07.032.